Search for Lorentz Invariance and *CPT* Violation with the MINOS Far Detector

P. Adamson,[9] D. J. Auty,[29] D. S. Ayres,[1] C. Backhouse,[23] G. Barr,[23] W. L. Barrett,[34] M. Bishai,[4] A. Blake,[6] G. J. Bock,[9] D. J. Boehnlein,[9] D. Bogert,[9] C. Bower,[14] S. Budd,[1] S. Cavanaugh,[11] D. Cherdack,[32] S. Childress,[9] B. C. Choudhary,[9] J. A. B. Coelho,[7] J. H. Cobb,[23] S. J. Coleman,[35] L. Corwin,[14] J. P. Cravens,[31] D. Cronin-Hennessy,[20] I. Z. Danko,[24] J. K. de Jong,[23,13] N. E. Devenish,[29] M. V. Diwan,[4] M. Dorman,[19] C. O. Escobar,[7] J. J. Evans,[19] E. Falk,[29] G. J. Feldman,[11] M. V. Frohne,[12,3] H. R. Gallagher,[32] R. A. Gomes,[10] M. C. Goodman,[1] P. Gouffon,[26] R. Gran,[21] N. Grant,[25] K. Grzelak,[33] A. Habig,[21] D. Harris,[9] P. G. Harris,[29] J. Hartnell,[29,25] R. Hatcher,[9] A. Himmel,[5] A. Holin,[19] X. Huang,[1] J. Hylen,[9] J. Ilic,[25] G. M. Irwin,[28] Z. Isvan,[24] D. E. Jaffe,[4] C. James,[9] D. Jensen,[9] T. Kafka,[32] S. M. S. Kasahara,[20] G. Koizumi,[9] S. Kopp,[31] M. Kordosky,[35] Z. Krahn,[20] A. Kreymer,[9] K. Lang,[31] G. Lefeuvre,[29] J. Ling,[27] P. J. Litchfield,[20] L. Loiacono,[31] P. Lucas,[9] W. A. Mann,[32] M. L. Marshak,[20] N. Mayer,[14] A. M. McGowan,[1] R. Mehdiyev,[31] J. R. Meier,[20] M. D. Messier,[14] D. G. Michael,[5,*] J. L. Miller,[36,*] W. H. Miller,[20] S. R. Mishra,[27] J. Mitchell,[6] C. D. Moore,[9] L. Mualem,[5] S. Mufson,[14] J. Musser,[14] D. Naples,[24] J. K. Nelson,[35] H. B. Newman,[5] R. J. Nichol,[19] W. P. Oliver,[32] M. Orchanian,[5] J. Paley,[1,14] R. B. Patterson,[5] T. Patzak,[8] G. Pawloski,[28] G. F. Pearce,[25] R. Pittam,[23] R. K. Plunkett,[9] J. Ratchford,[31] T. M. Raufer,[25] B. Rebel,[9] P. A. Rodrigues,[23] C. Rosenfeld,[27] H. A. Rubin,[13] V. A. Ryabov,[17] M. C. Sanchez,[15,1,11] N. Saoulidou,[9] J. Schneps,[32] P. Schreiner,[3] V. K. Semenov,[16] P. Shanahan,[9] W. Smart,[9] A. Sousa,[11] M. Strait,[20] N. Tagg,[22] R. L. Talaga,[1] J. Thomas,[19] M. A. Thomson,[6] G. Tinti,[23] R. Toner,[6] G. Tzanakos,[2] J. Urheim,[14] P. Vahle,[35] B. Viren,[4] A. Weber,[23] R. C. Webb,[30] C. White,[13] L. Whitehead,[4] S. G. Wojcicki,[28] D. M. Wright,[18] T. Yang,[28] M. Zois,[2] and R. Zwaska[9]

(MINOS Collaboration)

[1]*Argonne National Laboratory, Argonne, Illinois 60439, USA*
[2]*Department of Physics, University of Athens, GR-15771 Athens, Greece*
[3]*Physics Department, Benedictine University, Lisle, Illinois 60532, USA*
[4]*Brookhaven National Laboratory, Upton, New York 11973, USA*
[5]*Lauritsen Laboratory, California Institute of Technology, Pasadena, California 91125, USA*
[6]*Cavendish Laboratory, University of Cambridge, Madingley Road, Cambridge CB3 0HE, United Kingdom*
[7]*Universidade Estadual de Campinas, IFGW-UNICAMP, CP 6165, 13083-970, Campinas, SP, Brazil*
[8]*APC—Université Paris 7 Denis Diderot, 10, rue Alice Domon et Léonie Duquet, F-75205 Paris Cedex 13, France*
[9]*Fermi National Accelerator Laboratory, Batavia, Illinois 60510, USA*
[10]*Instituto de Física, Universidade Federal de Goiás, CP 131, 74001-970, Goiânia, GO, Brazil*
[11]*Department of Physics, Harvard University, Cambridge, Massachusetts 02138, USA*
[12]*Holy Cross College, Notre Dame, Indiana 46556, USA*
[13]*Physics Division, Illinois Institute of Technology, Chicago, Illinois 60616, USA*
[14]*Indiana University, Bloomington, Indiana 47405, USA*
[15]*Department of Physics and Astronomy, Iowa State University, Ames, Iowa 50011 USA*
[16]*Institute for High Energy Physics, Protvino, Moscow Region RU-140284, Russia*
[17]*Nuclear Physics Department, Lebedev Physical Institute, Leninsky Prospect 53, 119991 Moscow, Russia*
[18]*Lawrence Livermore National Laboratory, Livermore, California 94550, USA*
[19]*Department of Physics and Astronomy, University College London, Gower Street, London WC1E 6BT, United Kingdom*
[20]*University of Minnesota, Minneapolis, Minnesota 55455, USA*
[21]*Department of Physics, University of Minnesota–Duluth, Duluth, Minnesota 55812, USA*
[22]*Otterbein College, Westerville, Ohio 43081, USA*
[23]*Subdepartment of Particle Physics, University of Oxford, Oxford OX1 3RH, United Kingdom*
[24]*Department of Physics and Astronomy, University of Pittsburgh, Pittsburgh, Pennsylvania 15260, USA*
[25]*Rutherford Appleton Laboratory, Science and Technologies Facilities Council, OX11 0QX, United Kingdom*
[26]*Instituto de Física, Universidade de São Paulo, CP 66318, 05315-970, São Paulo, SP, Brazil*
[27]*Department of Physics and Astronomy, University of South Carolina, Columbia, South Carolina 29208, USA*
[28]*Department of Physics, Stanford University, Stanford, California 94305, USA*
[29]*Department of Physics and Astronomy, University of Sussex, Falmer, Brighton BN1 9QH, United Kingdom*
[30]*Physics Department, Texas A&M University, College Station, Texas 77843, USA*
[31]*Department of Physics, University of Texas at Austin, 1 University Station C1600, Austin, Texas 78712, USA*
[32]*Physics Department, Tufts University, Medford, Massachusetts 02155, USA*
[33]*Department of Physics, Warsaw University, Hoża 69, PL-00-681 Warsaw, Poland*
[34]*Physics Department, Western Washington University, Bellingham, Washington 98225, USA*

[35]Department of Physics, College of William & Mary, Williamsburg, Virginia 23187, USA
[36]Physics Department, James Madison University, Harrisonburg, Virginia 22807, USA
(Received 18 July 2010; published 4 October 2010)

We searched for a sidereal modulation in the MINOS far detector neutrino rate. Such a signal would be a consequence of Lorentz and *CPT* violation as described by the standard-model extension framework. It also would be the first detection of a perturbative effect to conventional neutrino mass oscillations. We found no evidence for this sidereal signature, and the upper limits placed on the magnitudes of the Lorentz and *CPT* violating coefficients describing the theory are an improvement by factors of 20–510 over the current best limits found by using the MINOS near detector.

DOI: 10.1103/PhysRevLett.105.151601 PACS numbers: 11.30.Cp, 14.60.Pq

Neutrinos have provided many crucial insights into particle physics, including the existence of physics beyond the minimal standard model with the detection of neutrino oscillations [1,2]. Because oscillations are interferometric in nature, they are sensitive to other indicators of new physics. Such indicators include potential small amplitude signals persisting to the current epoch whose origin is a fundamental theory that unifies quantum physics and gravity at the Planck scale $m_p \cong 10^{19}$ GeV. One promising category of Planck-scale signals is the violation of the Lorentz and *CPT* symmetries that are central to the standard model and general relativity. The standard-model extension (SME) is the comprehensive effective field theory that describes Lorentz (LV) and *CPT* violation (CPTV) at attainable energies [3].

The SME predicts behaviors for neutrino flavor change that are different from conventional neutrino oscillation theory. The probability of flavor change in the SME depends on combinations of L, the distance traveled by the neutrino, and the product of distance and the neutrino energy, $L \times E_\nu$. For conventional oscillation theory the transition probability depends only on L/E_ν. The SME also predicts that the neutrino flavor change probability depends on the angle between the direction of the neutrino and the LV/CPTV field in the Sun-centered inertial frame in which the SME is formulated [4]. Experiments like MINOS [5], whose neutrino beam is fixed on Earth, are well suited to search for this behavior, which would appear as a periodic variation in the detected neutrino rate as the beam swings around the field with the sidereal frequency $\omega_\oplus = 2\pi/(23^h56^m04.090\,53^s)$.

MINOS has a near detector (ND) located 1 km from the neutrino beam source and a far detector (FD) located 735 km from the neutrino source. Because of their different baselines, the ND and FD are sensitive to two separate limits of the general SME formulated for the neutrino sector. The predicted SME effects for baselines less than 1 km are independent of neutrino mass [4], and both MINOS [6] and LSND [7] reported searches for these effects. Recent theoretical work has shown that SME effects are a perturbation to the dominant mass oscillations for neutrinos having the appropriate L/E_ν to experience oscillations [8]. Since the probability for transitions due to LV increases with the baseline, experiments with baselines greater than ≈ 100 km are especially sensitive to LV and CPTV. The following analysis using MINOS FD data is the first search for perturbative LV and CPTV effects in an admixture with neutrino oscillations.

According to the SME, the transition probability for $\nu_\mu \to \nu_\tau$ transitions over long baselines is $P_{\mu\tau} \simeq P^{(0)}_{\mu\tau} + P^{(1)}_{\mu\tau}$, where $P^{(0)}_{\mu\tau}$ is the conventional mass oscillation probability for transitions between two flavors and $P^{(1)}_{\mu\tau}$ is the perturbation due to LV and CPTV, with $P^{(1)}_{\mu\tau}/P^{(0)}_{\mu\tau} \ll 1$. In the SME, $P^{(1)}_{\mu\tau}$ is given by [8]

$$P^{(1)}_{\mu\tau} = 2L\{(P^{(1)}_{\mathcal{C}})_{\tau\mu} + (P^{(1)}_{\mathcal{A}_s})_{\tau\mu}\sin\omega_\oplus T_\oplus + (P^{(1)}_{\mathcal{A}_c})_{\tau\mu}\cos\omega_\oplus T_\oplus + (P^{(1)}_{\mathcal{B}_s})_{\tau\mu}\sin 2\omega_\oplus T_\oplus + (P^{(1)}_{\mathcal{B}_c})_{\tau\mu}\cos 2\omega_\oplus T_\oplus\}, \quad (1)$$

where $L = 735$ km is the distance from neutrino production in the NuMI beam to the MINOS FD [2], $T_\oplus$ is the local sidereal time (LST) at neutrino detection, and the coefficients $(P^{(1)}_{\mathcal{C}})_{\tau\mu}$, $(P^{(1)}_{\mathcal{A}_s})_{\tau\mu}$, $(P^{(1)}_{\mathcal{A}_c})_{\tau\mu}$, $(P^{(1)}_{\mathcal{B}_s})_{\tau\mu}$, and $(P^{(1)}_{\mathcal{B}_c})_{\tau\mu}$ contain the LV and CPTV information. These coefficients depend on the SME coefficients that explicitly describe LV and CPTV, $(a_L)^\alpha_{\tau\mu}$ and $(c_L)^{\alpha\beta}_{\tau\mu}$, as well as the neutrino mass-squared splitting Δm^2_{32} [8]. For two-flavor transitions, only the real components of the $(a_L)^\alpha_{\tau\mu}$ and $(c_L)^{\alpha\beta}_{\tau\mu}$ contribute to the transition probability.

The magnitudes of the functions in Eq. (1) depend on the direction of the neutrino propagation in a fixed coordinate system on the rotating Earth. The direction vectors are defined by the colatitude of the NuMI beam line $\chi = (90^\circ \text{ latitude}) = 42.179\,733\,47^\circ$, the beam zenith angle $\theta = 86.7255^\circ$ defined from the z axis, which points up toward the local zenith, and the beam azimuthal angle $\phi = 203.909^\circ$ measured counterclockwise from the x axis chosen to lie along the detector's long axis.

This analysis selected data by using standard MINOS beam quality requirements and data quality selections [2,9]. The neutrino events used must interact in the 4.0 kt FD fiducial volume [9] and be charged-current (CC) in nature. The selection method described in Ref. [9] allowed

the identification of the outgoing muon in a CC interaction. As in Ref. [6], we focused on these events to maximize the ν_μ disappearance signal.

The data used come from the run periods listed in Table I; also shown are the number of protons incident on the neutrino production target (POT) for each period and the total number of events observed. To avoid biases, we performed the analysis blindly with the procedures determined by using only the runs I and II data. The run III data, comprising more than 50% of the total, were included only after finalizing the analysis procedures.

We tagged each neutrino event with the time determined by the Global Positioning System (GPS) receiver located at the FD site that reads out absolute universal coordinated time and is accurate to 200 ns [10]. The GPS time of the accelerator extraction magnet signal defined the time of each 10 μs beam spill. We converted the time of each neutrino event and spill to local sidereal time $T_\oplus$ (LST) in standard ways [11]. The uncertainty in the GPS time stamps introduced no significant systematic error into the analysis [6]. We placed each detected CC event into a histogram that ranged from 0 to 1 in the local sidereal phase (LSP), the LST of the event divided by the length of a sidereal day. We used the LSP for each spill to place the number of POTs for that spill, whether or not there was a neutrino event associated with it, into a second histogram. By dividing these two histograms, we obtained the normalized neutrino event rate as a function of the LSP, in which we searched for sidereal variations.

Since the search for sidereal variations used a fast Fourier transform (FFT) algorithm that works most efficiently for $\mathcal{N} = 2^n$ bins [12] and Eq. (1) puts power only into the Fourier terms $\omega_\oplus T_\oplus$ and $2\omega_\oplus T_\oplus$, we chose $\mathcal{N} = 2^4 = 16$ bins to retain these harmonic terms while still providing sufficient resolution in the sidereal phase to detect a sidereal signal. With this choice, each bin spanned 0.063 in the LSP or 1.5 hours in sidereal time.

The statistical similarity of the event rates for all runs was tested by comparing the rate for run i in LSP phase bin j, R_{ij}, with the weighted mean rate for that bin, $\bar{R}_j$. The distribution of $r = (R_{ij} - \bar{R}_j)/\sigma_{ij}$, where σ_{ij} is the statistical uncertainty in R_{ij} for all i and j, is Gaussian with $\bar{r} = 0$ and $\sigma = 1$, as expected for statistically consistent runs. Given this result, we combined the runs into a single data set whose rate as a function of the LSP is shown in Fig. 1. The mean rate is 2.36 ± 0.06 events per 10^{18} POTs, and the uncertainties shown in the figure are statistical.

TABLE I. Run parameters.

	Run dates	POTs	CC events
Run I	May05–Feb06	1.24×10^{20}	281
Run II	Sep06–Jul07	1.94×10^{20}	453
Run III	Nov07–Jun09	3.88×10^{20}	954

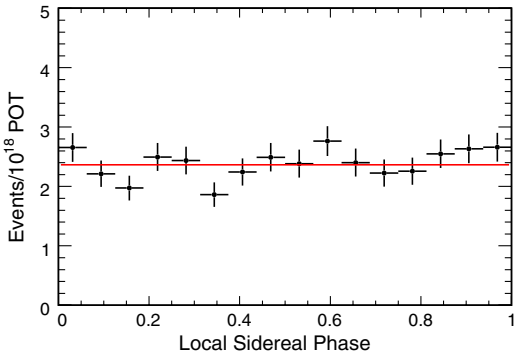

FIG. 1 (color online). Event rate as a function of the LSP for the total data set.

We searched for a sidereal signal by looking for excess power in the FFT of the data in Fig. 1 at the frequency corresponding to *exactly* 1 sidereal day. We used two statistics in our search: $p_1 = \sqrt{S_1^2 + C_1^2}$ and $p_2 = \sqrt{S_2^2 + C_2^2}$, where S_1^2 is the power returned by the FFT for $\sin(\omega_\oplus T_\oplus)$, C_1^2 is the power returned for $\cos(\omega_\oplus T_\oplus)$, and S_2^2 and C_2^2 are the analogous powers for the second harmonics. We used the quadratic sum of powers to minimize the effect of the arbitrary choice of zero point in the phase at 0^h LST. Table II gives the p_1 and p_2 values returned by the FFT for the total data set.

We determined the significance of our measurements of p_1 and p_2 by simulating 10^4 experiments without a sidereal signal. To construct these experiments we used the data themselves by randomizing the LSP of each CC event 10^4 times and placing each instance into a different phase histogram. We next randomized the LSP of each spill 10^4 times and placed the POT for each instance into another set of histograms. We drew the phases for each event and spill randomly from the LSP histogram of the start times for all spills. Dividing an event histogram by a POT histogram produced one simulated experiment. The randomization of both the spill and event LSPs removed any potential sidereal variation from the data.

We performed the FFT on the simulated experiments and computed the p_1 and p_2 statistics for each. The resulting distributions of p_1 and p_2 are nearly identical as shown in Fig. 2. The third column of Table II gives the probability $\mathcal{P}_F$ that the harmonic powers we found were due to statistical fluctuations. $\mathcal{P}_F$ is the probability of drawing a value of p_1 or p_2 from the parent distribution in Fig. 2 at least as large as found in the data.

TABLE II. Results for the p_1 and p_2 statistics from a FFT of the data in Fig. 1. The third column gives the probability $\mathcal{P}_\mathcal{F}$ that the measured value is due to a statistical fluctuation.

Statistic	p(FFT)	$\mathcal{P}_\mathcal{F}$
p_1	1.09	0.26
p_2	1.13	0.24

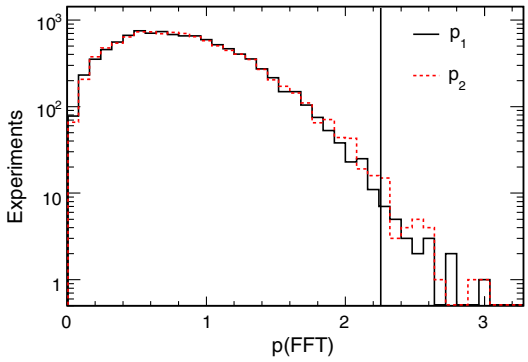

FIG. 2 (color online). Distributions of the p_1 and p_2 statistics from the FFT analysis of 10^4 simulated experiments without a sidereal signal. The adopted signal detection limit is $p(\mathrm{FFT}) = 2.26$.

The solid line at $p(\mathrm{FFT}) = 2.26$ in Fig. 2 divides the p_2 histogram at the point where 99.7% of the entries have lower values of the statistic. Consequently, we took $p(\mathrm{FFT}) = 2.26$ as the 99.7% confidence limit that a measured $p(\mathrm{FFT})$ for either harmonic indicates the distribution had no sidereal signal. That is, we adopted $p(\mathrm{FFT}) \geq 2.26$ as our signal detection threshold. Based on this threshold, the p_1 and p_2 statistics in Table II show no evidence for a sidereal signal. Thus, the normalized neutrino event rate exhibits no statistically significant variation that depends on the direction of the Earth-based neutrino beam in the Sun-centered inertial frame. In the context of the SME, this result is inconsistent with the detection of LV and CPTV.

We next determined the minimum detectable sidereal signal strength we could have found in this experiment by injecting a sidereal signal of the form $A\sin(\omega_\oplus T_\oplus)$, where A is a fraction of the mean event rate, into a new set of 10^4 simulated experiments and repeating the FFT analysis. We found that 68% of the experiments gave $p_1 \geq 2.26$ for $A = 9\%$. These simulations indicated that there was a 68% probability of detecting a sidereal modulation if the signal amplitude had been 9% of the mean event rate.

We tested the sensitivity of our results to several sources of systematic uncertainty. First we confirmed through simulated experiments that the analysis was insensitive to our choice of zero point in the phase, 0^h LST, due to the definition of p_1 and p_2. Next we tested sources that could introduce false sidereal signals into the data and mask an LV detection. Degradation of the NuMI target caused secular drifts of $\sim$5% in the neutrino production rate on a time scale of $\sim$6 months. Doubling this trend introduced no detectable signal for either secular decreases or increases. The daily variation in the detector response is on the order of 1% [2] and would not introduce a detectable sidereal variation into this analysis. The known $\pm 1.0\%$ uncertainty in the number of POTs per spill [2] was too small to affect this analysis. Because of the nonuniformity of the data taken throughout the solar year, diurnal effects, like temperature variations on the POT counting devices, could have introduced a false signal. However, systematic differences between the day and night event rates were smaller than the statistical errors in the rates themselves and could not introduce a false signal. Atmospheric effects could also have imprinted a sidereal signal on the data if there were a solar diurnal modulation in the event rate that beats with a yearly modulation [13]. Using methods described in Ref. [14], we found that this false sidereal signal is $<0.2\%$ of the mean event rate and well below the detection threshold.

Since we found no sidereal signal, we determined upper limits on the $(a_L)^\alpha_{\mu\tau}$ and $(c_L)^{\alpha\beta}_{\mu\tau}$ coefficients that describe LV and CPTV in the SME. Coefficients where both α and β are either T or Z cannot introduce a sidereal variation, and as such this experiment is not sensitive to them.

Neutrinos are simulated by using the standard MINOS Monte Carlo simulation [2] that models the NuMI beam line, including the hadron production and subsequent propagation through the focusing elements, hadron decay in the 675 m decay pipe, and the probability that any neutrinos produced will intersect the FD 735 km away. These neutrinos, along with weights determined by decay kinematics, are used in the detailed simulation of the FD. We chose $|\Delta m^2_{32}| = 2.43 \times 10^{-3}$ eV^2 and $\sin^2(2\theta_{23}) = 1$, the values measured by MINOS [2], for the simulation. Our tests show that changing these values within the allowed uncertainty does not alter the limits we found.

We determined the limits for each SME coefficient individually. We constructed a set of experiments in which one coefficient was set to be small but nonzero and the remaining coefficients were set to zero. We simulated a high statistics event histogram by picking events with a random sidereal phase drawn from the distribution of start times for the data spills and weighted these simulated events by both their survival probability and a factor to account for the different exposures between the data and the simulation. Simultaneously, we simulated a spill histogram by entering the average number of POTs required to produce one event in the FD, as determined from the data, at the sidereal phase of each simulated event. The division of these two histograms resulted in the LSP histogram we used to compute the p_1 and p_2 statistics. We then increased the magnitude of the nonzero SME coefficient and repeated the process until either p_1 or p_2 was greater than the 2.26 detection threshold. To reduce fluctuations we computed the limit 100 times and averaged the results. Table III gives the mean magnitude of the coefficient required to produce a signal above threshold. This procedure could miss fortuitous cancellations of SME coefficients. We did not consider these cases. We cross-checked these limits by simulating 750 low statistics experiments for each coefficient limit given in Table III. Each experiment had the same total number of neutrinos as the data and thus represents the statistical fluctuations in the data. The distributions of the p_1 and p_2 statistics for all the experiments were used to determine

TABLE III. 99.7% C.L. limits on SME coefficients for $\nu_\mu \to \nu_\tau$; $(a_L)^\alpha_{\mu\tau}$ have units [GeV]; $(c_L)^{\alpha\beta}_{\mu\tau}$ are unitless. The columns labeled $\mathcal{I}$ show the improvement from the near detector limits.

Coeff.	Limit	$\mathcal{I}$	Coeff.	Limit	$\mathcal{I}$
$(a_L)^X_{\mu\tau}$	5.9×10^{-23}	510	$(a_L)^Y_{\mu\tau}$	6.1×10^{-23}	490
$(c_L)^{TX}_{\mu\tau}$	0.5×10^{-23}	20	$(c_L)^{TY}_{\mu\tau}$	0.5×10^{-23}	20
$(c_L)^{XX}_{\mu\tau}$	2.5×10^{-23}	220	$(c_L)^{YY}_{\mu\tau}$	2.4×10^{-23}	230
$(c_L)^{XY}_{\mu\tau}$	1.2×10^{-23}	230	$(c_L)^{YZ}_{\mu\tau}$	0.7×10^{-23}	170
$(c_L)^{XZ}_{\mu\tau}$	0.7×10^{-23}	190	...	...	...

the confidence level at which the measured values in Table II are excluded by each limit. The exclusion using this method is >99.7% C.L. for all coefficients.

In summary, we found no evidence for sidereal variations in the neutrino rate in the MINOS FD. This result, when framed in the SME [4,8], leads to the conclusion that we have detected no evidence for the violation of Lorentz or *CPT* invariance described by this framework for neutrinos traveling over the 735 km baseline from their production in the NuMI beam to the MINOS FD. The limits on the SME coefficients in Table III for the FD that come from this null result improve the limits we found for the ND by factors of the order of 20–510 [6]. This improvement is due to the different behavior of the oscillation probability in the short and long baseline approximations coupled with the significantly increased baseline to the FD. These improvements more than offset the significant decrease in statistics in the FD. They are the first limits to be determined for the neutrino sector in which LV and CPTV are assumed to be a perturbation on the conventional neutrino mass oscillations.

We gratefully acknowledge the many valuable conversations with Alan Kostelecký and Jorge Diaz during the course of this work. This work was supported by the U.S. DOE, the United Kingdom STFC, the U.S. NSF, the State and University of Minnesota, the University of Athens, Greece, and Brazil's FAPESP and CNPq. We are grateful to the Minnesota Department of Natural Resources, the crew of the Soudan Underground Laboratory, and the staff of Fermilab for their contribution to this effort.

*Deceased.

[1] R. Becker-Szendy *et al.* (IMB-3 Collaboration), Phys. Rev. D **46**, 3720 (1992); K. S. Hirata *et al.* (Kamiokande Collaboration), Phys. Lett. B **280**, 146 (1992); Y. Fukuda *et al.* (Super-Kamiokande Collaboration), Phys. Rev. Lett. **81**, 1562 (1998); W. W. M. Allison *et al.* (Soudan-2 Collaboration), Phys. Rev. D **72**, 052005 (2005); M. Ambrosio *et al.* (MACRO Collaboration), Eur. Phys. J. C **36**, 323 (2004); K. Abe *et al.* (Super-Kamiokande Collaboration), Phys. Rev. Lett. **97**, 171801 (2006); S. Abe *et al.* (KamLAND Collaboration), Phys. Rev. Lett. **100**, 221803 (2008).

[2] D. G. Michael *et al.*, Phys. Rev. Lett. **97**, 191801 (2006); P. Adamson *et al.* (MINOS Collaboration), Phys. Rev. D **77**, 072002 (2008); Phys. Rev. Lett. **101**, 131802 (2008).

[3] D. Colladay and V. A. Kostelecký, Phys. Rev. D **55**, 6760 (1997); **58**, 116002 (1998); V. A. Kostelecký, Phys. Rev. D **69**, 105009 (2004); G. Amelino-Camelia *et al.*, AIP Conf. Proc. **758**, 30 (2005); R. Bluhm, Lect. Notes Phys. **702**, 191 (2006); V. A. Kostelecký and N. Russell, arXiv:0801.0287.

[4] V. A. Kostelecký and M. Mewes, Phys. Rev. D **69**, 016005 (2004).

[5] D. G. Michael *et al.* (MINOS Collaboration), Nucl. Instrum. Methods Phys. Res., Sect. A **596**, 190 (2008).

[6] P. Adamson *et al.* (MINOS Collaboration), Phys. Rev. Lett. **101**, 151601 (2008).

[7] L. B. Auerbach *et al.* (LSND Collaboration), Phys. Rev. D **72**, 076004 (2005).

[8] J. S. Diaz, V. A. Kostelecky, and M. Mewes, Phys. Rev. D **80**, 076007 (2009).

[9] P. Adamson *et al.* (MINOS Collaboration), Phys. Rev. Lett. **101**, 221804 (2008); Phys. Rev. D **81**, 052004 (2010).

[10] P. Adamson *et al.* (MINOS Collaboration), Phys. Rev. D **76**, 072005 (2007).

[11] P. Duffett-Smith, *Practical Astronomy with Your Calculator* (Cambridge University Press, Cambridge, England, 1992).

[12] W. H. Press *et al.*, *Numerical Recipes in C* (Cambridge University Press, Cambridge, England, 1999).

[13] A. Compton and I. Getting, Phys. Rev. **47**, 817 (1935).

[14] M. Ambrosio *et al.*, Phys. Rev. D **67**, 042002 (2003).